Chemical Engineering Journal 158 (2010) 154–166

Contents lists available at ScienceDirect

Chemical Engineering Journal

journal homepage: www.elsevier.com/locate/cej

Degradation of chlorinated hydrocarbons by UV/H_2O_2: The application of experimental design and kinetic modeling approach

Petra Kralik, Hrvoje Kusic*, Natalija Koprivanac, Ana Loncaric Bozic**

Faculty of Chemical Engineering and Technology, University of Zagreb, Marulicev trg 19, Zagreb 10000, Croatia

ARTICLE INFO

Article history:
Received 25 October 2009
Received in revised form 2 December 2009
Accepted 12 December 2009

Keywords:
Chlorinated hydrocarbons
p-Chlorophenol
UV/H_2O_2
Experimental design
Kinetic modeling

ABSTRACT

The aim of the study was to develop a detail mathematical model describing the degradation of chlorinated hydrocarbon pollutants in water by UV/H_2O_2 process. As a model representative of chlorinated hydrocarbons *para*-chlorophenol (*p*-CP) was chosen. A degradation mechanism of parent pollutant to its aromatic and aliphatic by-products, as well as the mineralization of simulated wastewater, was included in the model. The optimal values of operating parameters of UV/H_2O_2 process influencing the treatment efficiency were established by the means of the two-factor three-level Box–Behnken experimental design combining with response surface modeling (RSM) and quadratic programming. The results of such experimental design using different statistical tools showed that pH 6.8 and pollutant/oxidant ratio 1:199 maximize the performance of oxidative treatment system. The model was tested to evaluate accuracy in predicting system behavior at different process conditions and pollutant concentrations. Rather high accuracy of developed model was demonstrated at all tested conditions. Good accordance of the data predicted by model and the empirically obtained data was confirmed by calculated standard deviation (SD) for each experimentally monitored parameter. Hence, the developed mathematical model describing the kinetic of *p*-CP degradation by UV/H_2O_2 can be characterized as interpretable, transparent and accurate, and therefore can be used as a tool for maximizing efficiency of wastewater treatment process.

1. Introduction

The sizable fraction of overall organic chemical compounds produced annually worldwide and used by various industries such as chemical, agriculture, pharmaceutical, food, dyestuff, petrochemical, etc. pertain to chlorinated hydrocarbons. These compounds, when released in the environment over industrial exhausting gases or wastewater streams, present direct and serious threat to all living organisms in aquatic systems and soil [1,2]. One of the typical representatives of the group of chlorinated hydrocarbons pollutants, possessing a great potential for high environmental risk and public concern are chlorophenols (CPs); introduced into the environment as a result of several man-made activities, e.g. water disinfection, waste incineration, uncontrolled used of pesticides and herbicides, as well as by-products in bleaching of paper pulp with chlorine [3,4]. CPs are designated as the priority pollutants by the U.S. EPA [5] and European Commission [6]. According to the European Pollutant Emissions Register, their direct and indirect releases to waters in Europe are estimated to more than 1300 tones in 2003 [7]. The most of CPs are hardly biodegradable and also difficult to remove from the environment, thus increasing their hazardous potential to the environment due to the proven toxicity and suspected carcinogenicity as well [8].

Due to the low biodegradability of CPs [4], as well the shortcomings of insufficiently effective common wastewater treatment technologies, particularly physical and chemical–physical methods transferring the pollution from one phase to another causing the demand for secondary treatment [4,9,10], the alternative treatment technologies, such as advanced oxidation technologies (AOPs) have received increased interest [4,11]. AOPs are destructive, low- or non-waste conversion technologies involving the generation of hydroxyl radicals in sufficient quantities to oxidize the majority of organics present in the water matrix [11,12]. Among various types and combinations of AOPs, the chemical and photochemical processes based on usage of either Fenton type reagent or photooxidation alongside H_2O_2 are shown to be suitable for the degradation of phenols in water [11–20]. Although efficient and cost effective, the problem often rising from the application of Fenton type processes is the relatively high concentration of iron ions in the bulk after the treatment which may demand a secondary treatment. In this study, the UV/H_2O_2 process is considered for the degradation and mineralization of *p*-CP in water matrix. It is worth of noting that all AOPs, including UV/H_2O_2 process, are multifactor systems. For

* Corresponding author. Tel.: +385 1 4597 160; fax: +385 1 4597 143.
** Corresponding author. Tel.: +385 1 4597 123; fax: +385 1 4597 143.
E-mail addresses: hkusic@fkit.hr (H. Kusic), abozic@fkit.hr (A. Loncaric Bozic).

1385-8947/$ – see front matter © 2009 Elsevier B.V. All rights reserved.
doi:10.1016/j.cej.2009.12.023

this reason the characterization of such system requires taking into consideration not only single-factor effects, which was done in the above-mentioned studies and our previous work, but also the cross-factor effects. The cross-factor experimental design methodology used in this study is a valuable tool to overcome the limits of long lasting experimental studies. Besides experimental design which is highly important due to the fact that AOPs are highly sensitive to the particular types of pollutants and might demand different process conditions, the development of detail mathematical model predicting the degradation of organics by AOPs, in this case by UV/H_2O_2, is one of the most important issues to be solved prior to the scale-up to pilot and large scale treatment application.

Considering all above stated, the effects of operational parameters of UV/H_2O_2 process, pH and pollutant/oxidant ratio, for the degradation of *p*-CP in water matrix was investigated and their optimal values were determined and verified by the means of two-factor three-level Box–Behnken experimental design combined with response surface modeling (RSM) and quadratic programming. The main goal of the study was to develop the detailed mathematical model predicting system behavior, i.e. degradation of *p*-CP by UV/H_2O_2. The intention was to develop a model which would predict not only conversion of parent pollutant, but also the formation and subsequent degradation of its by-products, both aromatic and aliphatic, up to the formation of final inorganic products of *p*-CP mineralization. Such model could be used for prediction of system behavior operated at different conditions with the aim of maximizing efficiency of wastewater treatment process.

2. Experimental

2.1. Chemicals

All organic chemicals used in the study: *p*-chlorophenol (*p*-CP), 4-chlorocatechol (4Cl-CC), phenol (PH), hydroquinone (HQ), benzoquinone (BQ), maleic acid (MaleAc), fumaric acid (FumAc), succinic acid (SucAc), malonic acid (MaloAc), oxalic acid (OxAc), acetic acid (AcAc), formic acid (FoAc) and methanol (MeOH) were at least of GC grade or higher purity and were purchased by Sigma–Aldrich, USA. The inorganic chemicals used either as an oxidant (hydrogen peroxide (H_2O_2), $w = 30\%$) or as HPLC mobile phase (*ortho*-phosphoric acid (*o*-H_3PO_4), $w \approx 85\%$) or as auxiliary chemicals for initial pH values adjustment (NaOH, p.a. and H_2SO_4, >96%) were also purchased by Sigma–Aldrich. All experiments were performed with deionized water with conductivity less than 1 $\mu S\,cm^{-1}$, which was also used for preparing all calibration standard solutions.

2.2. Experimental procedure

All experiments were performed in the glass water-jacketed batch reactor, which was described in details in our previous studies [19,20], while only the brief description is given in following text. The UV lamp emitting irradiation in UV-C region (typical intensity on 2 cm ≈ 4.4 mW cm^{-2}) was located in the middle of the reactor in a quartz tube. The value of incident photon flux at 254 nm, $I_0 = 3.68 \times 10^{-6}$ Einstein s^{-1}, was calculated on the basis of hydrogen peroxide actinometry measurements [21] and it is described in details elsewhere [22]. The total volume of the treated solution was 0.5 L, while the mixing was provided by magnetic stirring bar. Temperature was maintained at 25 ± 0.2 °C by circulating the water through the jacket around the photoreactor. Initial pH values and hydrogen peroxide concentration ranged from 5 to 9 and 50 mM to 150 mM, respectively, in order to achieve requirements for the desired three-level Box–Behnken design. Initial pH was adjusted with the addition of 0.1 M NaOH or 0.1 M H_2SO_4. Added quantities of H_2SO_4, NaOH and H_2O_2 as an oxidizing agent, were negligible in comparison to the total volume of treated reaction mixture. The duration of each experiment was 60 min; samples were taken periodically from the reactor (0, 5, 10, 15, 20, 25, 30, 35, 40, 45, 50, 55, 60) and thereafter immediately analyzed. All experiments were repeated at least three times and averages were reported, while reproducibility of the experiments was within 5%.

2.3. Analyses

The decomposition of *p*-CP and the formation of its primary aromatic by-products such as 4Cl-CC, PH, HQ and BQ, as well as their further degradation to aliphatic intermediates such as MaleAc, FumAc, SucAc, MaloAc, AcAc, OxAc and FoAc were analyzed by HPLC, Shimadzu, Japan, equipped with diode-array UV detector, SPD-M10A_{VP}, Shimadzu, Japan. The monitoring of aromatic species was performed using a 5 μm, 25.0 cm × 4.6 mm, Supelco Discovery C18 column, USA, with mobile phase H_2O/MeOH at flow 1.0 mL min^{-1} operated by binary gradient method changing MeOH percentage from 32% to 60%. Aliphatic by-products were monitored using 9 μm, 25.0 cm × 4.6 mm, SUPELCOGEL-H column, USA, with 0.1% *o*-H_3PO_4 as mobile phase operated with isocratic method at 0.2 mL min^{-1}. The residual *p*-CP was reported as a normalized value, [*p*-CP]/[*p*-CP]$_0$, while all its formed by-products, either aromatics or aliphatics, were reported relatively to initial *p*-CP concentration, e.g. [HQ]/[*p*-CP]$_0$, taking into account the stoichiometric ratio in the cases of lower C-atomic species. The measurement of total organic content during experiments was performed using Total Organic Carbon analyzer, TOC-V_{CPN}, Shimadzu, Japan. Handylab pH/LF portable pH-meter, Schott Instruments GmbH, Mainz, Germany, was used for pH measurements. The consumption of hydrogen peroxide during the treatment of *p*-CP model wastewater was monitored using modified iodometric titration method [23].

3. Model formulation

3.1. Response surface methodology and statistical analysis

In order to verify optimal conditions, pH range and pollutant/oxidant ratio, for the maximal efficiency of *p*-CP degradation by UV/H_2O_2 in water matrix the two-factor three-level Box–Behnken experimental design combined with response surface modeling (RSM) and quadratic programming was used. RSM consists of a group of empirical techniques devoted to the evaluation of relationships existing between a cluster of controlled experimental factors and measured responses according to one or more selected criteria [24,25]. In the first step of RSM, a suitable approximation is introduced to find true relationship between the dependent variable (response) and the set of independent variables (factors). If knowledge concerning the shape of true response surface is insufficient, the preliminary model (generally a first-order model) is upgraded by adding high-order terms to it [24]. In the next step, the behavior of the system is explained by the following quadratic equation [24–26]:

$$Y = \beta_0 + \sum_{i=1}^{k} \beta_i X_i + \sum_{i=1}^{k} \beta_{ii} {X_i}^2 + \sum_{i=1}^{k} \sum_{j=1}^{k} \beta_{ij} X_i X_j + \varepsilon' \quad (1)$$

where Y states for the process response or output, i.e. dependent variable; k represents the number of patterns; i and j are index numbers for patterns; β_0 is the free, i.e. offset term, $X_i \ldots X_k$ are coded independent variables; β_i is the first-order, i.e. linear, main effect; β_{ii} is the quadratic, i.e. squared, effect; while β_{ij} represents the interaction effect and ε' is the random error allowing the discrepancies or uncertainties between predicted and observed values.

Table 1
Box–Behnken design matrix with two independent variables expressed in coded and natural units, and values of obtained responses.

Runs	Variables				Responses			
	Variable1, X_1		Varariable2, X_2		Response1, Y_1		Response2, Y_2	
	Level	Actual value: pH_0	Level	Actual value: $[H_2O_2]$, mM	k of p-CP decay, $\times10^{-3}$ s^{-1}		TOC removal, norm	
					Observed	Predicted	Observed	Predicted
1	−1	5	−1	50	0.68	0.73	0.149	0.143
2	−1	5	0	100	0.91	0.91	0.224	0.230
3	−1	5	1	150	0.66	0.61	0.139	0.138
4	0	7	−1	50	0.76	0.76	0.159	0.173
5	0	7	0	100	1.03	0.94	0.284	0.261
6	0	7	1	150	0.55	0.64	0.160	0.169
7	1	9	−1	50	0.81	0.76	0.136	0.127
8	1	9	0	100	0.87	0.95	0.198	0.215
9	1	9	1	150	0.68	0.64	0.131	0.123

When developing the model presented by Eq. (1), the natural, i.e. uncoded, independent variables should be transformed in dimensionless coded values at three levels −1, 0 and 1. In such manner, the chosen effects in the study influencing the degradation of p-CP by UV/H_2O_2 process are the initial pH value (X_1) and the concentration of H_2O_2 (X_2). Besides their influence on the pseudo-first-order decay rate of p-CP as a first response (Response1), the influence of chosen process parameters was also tested on the mineralization degree of p-CP simulated wastewater after 60 min treatment period (Response2). The experimental range and levels of independent variables considered in this study, including also observed and predicted values of both responses by developed quadratic models are presented in Table 1. The fitting of models was calculated using the coefficient of determination R-squared (R^2) and the analysis of variance. The Box–Behnken method was selected for designing the experiments due to the fact that rather few combinations of the variables are required to estimate a potentially complex response function [27]. In total, only nine experiments were found to be sufficient to calculate the six coefficients of the second-order polynomial regression (quadratic) model. For the purpose of anal-

Table 2
The reactions, rate constants and quantum yields used for the kinetic modeling.

#	Reaction	Ref.	k (M^{-1} s^{-1})	
			Lit.	Used
1	$H_2O_2 + h\nu \rightarrow 2OH^\bullet$	[13,20,30,31]	Φ = 0.5 mol Ein^{-1}	Φ = 0.5 mol Ein^{-1}
2	$OH^\bullet + H_2O_2 \rightarrow HO_2^\bullet + H_2O$	[20,31–33]	$1.2–4.5 \times 10^7$	4.5×10^7
3	$OH^\bullet + HO_2^- \rightarrow HO_2^\bullet + OH^-$	[13]	7.5×10^9	7.5×10^9
4	$HO_2^\bullet + H_2O_2 \rightarrow H_2O + HO^\bullet + O_2$	[13]	3.0	3.0
5	$O_2^{\bullet-} + H_2O_2 \rightarrow OH^- + HO^\bullet + O_2$	[13]	0.13	0.13
6	$2OH^\bullet \rightarrow H_2O_2$	[20,31,33]	$4.2–5.3 \times 10^9$	5.3×10^9
7	$HO_2^\bullet + OH^\bullet \rightarrow H_2O + O_2$	[20,31,33]	1×10^{10}	1×10^{10}
8	$2HO_2^\bullet \rightarrow H_2O_2 + O_2$	[20,31,33]	8.3×10^5	8.3×10^5
9	$O_2^{\bullet-} + HO_2^\bullet \rightarrow HO_2^- + O_2$	[20,31,33]	9.7×10^7	9.7×10^7
10	$O_2^{\bullet-} + HO^\bullet \rightarrow HO^- + O_2$	[33]	1.0×10^{10}	1×10^{10}
11	$HO_2^\bullet \rightarrow O_2^{\bullet-} + 2H^+$	[20,31,33]	$1.58–7.9 \times 10^5$ s^{-1}	1.58×10^5 s^{-1}
12	$O_2^{\bullet-} + 2H^+ \rightarrow HO_2^\bullet$	[20,31,33]	1.0×10^{10}	1.0×10^{10}
13	$OH^\bullet + H_2O_2 \rightarrow O_2^{\bullet-} + H_2O$	[33]	2.7×10^7	2.7×10^7
14	$HO_2^- + H^+ \rightarrow H_2O_2$	[22,34]	2.6×10^{10}	2.6×10^{10}
15	$H_2O_2 \rightarrow HO_2^- + H^+$	[22,34]	3.7×10^{-2}	3.7×10^{-2}
16	$HO^- + H^+ \rightarrow H_2O$	[22,34]	1.4×10^{11}	1.4×10^{11}
17	$H_2O \rightarrow HO^- + H^+$	[22,34]	2.5×10^{-5}	2.5×10^{-5}
18	$p\text{-CP} + h\nu \Leftrightarrow z_1\text{Cl-CC} + z_2\text{HQ} + z_3\text{UnBP}$	[35]	Φ = 0.017 mol Ein^{-1}	Φ = 0.059 mol Ein^{-1}
19	$p\text{-CP} + OH^\bullet \rightarrow q_1\text{Cl-CC} + q_2\text{HQ} + q_3\text{UnBP}$	[36] [37]	9.3×10^9 at pH 6 7.6×10^9 at pH 9	9.3×10^9 at pH 6 7.6×10^9 at pH 9
20	$\text{Cl-CC} + h\nu \Leftrightarrow \text{UnBP}$			Φ = 0.057 mol Ein^{-1}
21	$\text{Cl-CC} + OH^\bullet \rightarrow w_1\text{MaleAc} + w_2\text{FumAc} + w_3\text{MaloAc}$	[36]	7.0×10^9	7.0×10^9
22	$\text{HQ} + h\nu \Leftrightarrow e_1\text{FumAc} + e_2\text{UnBP}$			Φ = 0.047 mol Ein^{-1}
23	$\text{HQ} + OH^\bullet \rightarrow w_1\text{MaleAc} + w_2\text{FumAc} + w_3\text{MaloAc}$	[38]	5.2×10^9	5.2×10^9
24	$\text{MaleAc} + h\nu \Leftrightarrow \text{FumAc}$			Φ = 0.020 mol Ein^{-1}
25	$\text{MaleAc} + OH^\bullet \rightarrow n_1\text{OxAc} + n_2\text{FoAc}$	[39]	6.0×10^9	6.0×10^9
26	$\text{FumAc} + h\nu \Leftrightarrow \text{MaleAc}$			Φ = 0.028 mol Ein^{-1}
27	$\text{FumAc} + OH^\bullet \rightarrow n_1\text{OxAc} + n_2\text{FoAc}$	[39]	6.0×10^9	6.0×10^9
28	$\text{MaloAc} + OH^\bullet \rightarrow \text{OxAc}$	[40,41]	$1.6–2.4 \times 10^7$	1.28×10^9
29	$\text{OxAc} + h\nu \Leftrightarrow \text{IP}$			Φ = 0.006 mol Ein^{-1}
30	$\text{OxAc} + OH^\bullet \rightarrow \text{IP}$	[42]	1.4×10^6	1.4×10^6
31	$\text{FoAc} + OH^\bullet \rightarrow \text{IP}$	[43]	1.3×10^8	1.3×10^8
32	$\text{UnBP} + OH^\bullet \rightarrow m_1\text{OxAc} + m_2\text{FoAc} + m_3\text{IP}$			6.83×10^9
33	$\text{ArBP} + OH^\bullet \rightarrow \text{AlBP}$			6.25×10^9
34	$\text{AlBP} + OH^\bullet \rightarrow \text{IP}$			5.83×10^8
35	$\text{OC} + OH^\bullet \rightarrow \text{IP}$	[20]	2.33×10^8	2.22×10^8

p-CP: *para*-chlorophenol; Cl-CC: 4-chlorocatechol; HQ: hydroquinone; MaleAc: maleic acid; FumAc: fumaric acid; MaloAc: malonic acid; OxAc: oxalic acid; FoAc: formic acid; UnBP: unidentified by-products; IP: inorganic products (i.e. mineralized part of p-CP solution); ArBP: aromatic by-products; AlBP: aliphatic by-products; and e_1, e_2, m_1, m_2, m_3, n_1, n_2, q_1, q_2, q_3, w_1, w_2, w_3, z_1, z_2, z_3: fraction coefficients.

Table 3
Analysis of variance (ANOVA) of the response surface model for the prediction of Response1, pseudo-first-order rates of *p*-CP decay, k ($\times 10^{-3}$ s^{-1}), including the multiple regression results and significance of the components for the quadratic model ($R^2 = 0.8465$, $R^2_{adj} = 0.5906$).

Factors (coded)	Statistics					Model results				
	SS	d.f.	MSS	F	p	Parameter	Coefficient	Effect	SE	t
Model	0.1489	5	0.0298	3.3083	0.1431					
Intercept						β_0	0.9444			
X_1	0.0020	1	0.0020	0.2245	0.6680	β_1	0.0183	0.0367	0.0774	0.4738
X_1^2	0.0003	1	0.0003	0.0303	0.8729	β_{11}	−0.0117	−0.0117	0.0670	0.1741
X_2	0.0216	1	0.0216	2.4042	0.2188	β_2	−0.0600	−0.1200	0.0774	−1.5506
X_2^2	0.1217	1	0.1217	13.5447	0.0348*	β_{22}	−0.2467	−0.2467	0.0670	3.6803
$X_1 \times X_2$	0.0030	1	0.0030	0.3367	0.6025	β_{12}	−0.0275	−0.0550	0.0948	−0.5803
Error	0.0267	3	0.0090							
Total	0.1756	8								

* $p < 0.05$ is considered as significant.

ysis of variance (ANOVA), regression and graphical analyses of the obtained data a software package STATISTICA 9.0, StatSoft Inc., USA, was used. Some statistical parameters were also calculated using to on-line statistical calculators: one by P. Kuzmic from BioKin Ltd., USA [28], and another by Prof. D.S. Soper from California State University [29]. The optimal values of studied process parameters predicted by RSM were calculated using numerical technique built-in software *Mathematica 6.0* (Wolfram Research, Champaign, IL).

3.2. Development of mathematical model predicting p-CP degradation

The mathematical model (M1) for predicting *p*-CP degradation by UV/H_2O_2 process, including 19 chemical species (ions, atoms and molecules) and 32 chemical reactions, was developed using chemical reactions and rate constants mostly from literature (Table 2) [13,20,22,30–43]. The general mass balance for a well-mixed, constant volume and constant temperature batch reactor is given by:

$$\frac{dc_i}{dt} = -r_i \quad (2)$$

where c_i is concentration of specie i in the bulk and r_i is the bulk phase rate of the same specie [44]. *p*-CP degradation was simulated by *Mathematica 6.0* (Wolfram Research, Champaign, IL) using GEAR method which finds the numerical solution to the set of ordinary differential equations. Alongside detailed M1 model, the auxiliary model M2 describing the degradation of *p*-CP in water matrix by direct photolysis is developed separately and incorporated in M1. Quantum yields of monitored organics as well as fraction coefficients where determined on the basis of experimentally obtained results in the following manner. Quantum yields are determined by trial and error method inserting the values into the modified version of semiempirical "LL model" based on the Lambert's law (3) [30]:

$$r_{UV} = -\frac{dc_i}{dt} = \Phi_i \times F_i \times I_0 \times (1 - \exp(-2.303 \times L \times \sum \varepsilon_j \times c_j)) \quad (3)$$

being $F_i = (\varepsilon_i \times c_i)/(\sum \varepsilon_j \times c_j)$

Other constants presented in above Eq. (4), Φ_i, ε_i, I_0 and L, stand for the physical properties of specie i, its quantum yield and the extinction coefficient, the incident photon flux by reactor volume unit and the effective optical path in the reactor, respectively. Taking into the consideration only the beginning of the photolysis process, it can be assumed that almost all radiation was absorbed by the parent compound i. In the latter case, it follows that $\varepsilon_i \times c_i \approx \varepsilon_j \times c_j$ and $F_i \approx 1$. Consequently, Eq. (4) could be modified into following expression [35].

$$r_{UV} = -\frac{dc_i}{dt} = \Phi_i \times I_0 \times (1 - \exp(-2.303 \times L \times \varepsilon_i \times c_i)) \quad (4)$$

Knowing the values of I_0 and L, the quantum yield of the specie i could be calculated, as it was done in our case for all monitored organics, either parent pollutant or its degradation by-products (Table 2, #1, 18, 20, 22, 24, 26 and 29). The fraction coefficients e, m, n, q, w and z, representing the fraction of particular monitored organic compound degrading to its intermediates, were determined by trial and error method fitting the values into the model with simultaneous comparison with experimental data, minimizing the value of standard deviation. Observed discrepancy between monitored TOC value and the sum TOC calculated from the concentration of monitored organics is contributed to the formation of unidentified by-products, UnBP. The rate constant of reaction *#32* (Table 2) was determined in above explained manner. Also, the sum model M3 was developed by taking into account reactions typical for UV/H_2O_2 process (Table 2, *#1–17*) and the simplified mechanism of *p*-CP degradation to the inorganic products (IP) presented by Eq. (5), where ArBP and AlBP stand for sum of aromatic and aliphatic by-products, respectively.

$$p\text{-CP} + HO^\bullet \rightarrow ArBP + HO^\bullet \rightarrow AlBP + HO^\bullet \rightarrow IP \quad (5)$$

4. Results and discussion

4.1. Experimental design

In order to study the influence of UV/H_2O_2 process parameters, initial operating pH and pollutant/oxidant ratio, the experimental design based on Box–Behnken two-factors three-level model was performed. In this study, pH range 5–9 and pollutant/oxidant ratio 1:100–1:300 were taken into the consideration as favorable for the degradation of phenolic compounds due to the knowledge from the literature and the findings from our previous work [16–19]. The influence of both studied process parameters was observed on two responses: "pseudo"-first-order decay rate of *p*-CP (k, 10^{-3} s^{-1}) and mineralization extent of *p*-CP model wastewater (TOC removal, norm) after one hour treatment. In Table 1 the Box–Behnken statistical combinations taken into the calculation are summarized, as well as the observed and predicted responses for both k and TOC removal. The usage of response surface methodology (RSM) is based on the estimation of parameters which indicate an empirical relationship between the response and the input variables (Eq. (1)). The RSM gave the following fitted second-order polynomial equation in the case of Response1, "pseudo"-first-order decay rate of *p*-CP (6):

$$Y_1 = 0.9444 + 0.0183 \times X_1 - 0.0117 \times X_1^2 - 0.0600 \times X_2 - 0.2467 \times X_2^2 - 0.0275 \times X_1 X_2 \quad (6)$$

where Y_1 is the predicted k of *p*-CP decay, X_1 and X_2 are coded terms for two independent test variables, presenting pH and H_2O_2 concentration, respectively. According to the several authors

Table 4
Analysis of variance (ANOVA) of the response surface model for the prediction of Response2, TOC removal (norm), including the multiple regression results and significance of the components for the quadratic model (R^2 = 0.9364, R^2_{adj} = 0.8304).

Factors (coded)	Statistics					Model results				
	SS	d.f.	MSS	F	p	Parameter	Coefficient	Effect	SE	t
Model	0.0194	5	0.0039	9.7000	0.0357*					
Intercept						β_0	0.2608			
X_1	0.0004	1	0.0004	0.8383	0.4274	β_1	−0.0078	−0.0157	0.0171	−0.9156
X_1^2	0.0029	1	0.0029	6.6338	0.0821	β_{11}	−0.0382	−0.0382	0.0148	2.5756
X_2	3.3×10^{-5}	1	3.3×10^{-5}	0.0744	0.8028	β_2	−0.0023	−0.0047	0.0171	−0.2727
X_2^2	0.0161	1	0.0161	36.6145	0.0091*	β_{22}	−0.0897	−0.0897	0.0148	6.0510
$X_1 \times X_2$	6.3×10^{-6}	1	6.3×10^{-6}	0.0142	0.9126	β_{12}	0.0013	0.0025	0.0210	0.1193
Error	0.0013	3	0.0004							
Total	0.0207	8								

* $p < 0.05$ is considered as significant.

[26,45–47], the analysis of variance is considered to be essential to test the significance of the model. Hence, the ANOVA was performed in order to test the significance of the fit of the second-order polynomial model (Eq. (6)) predicting the *p*-CP decay in dependence of used process conditions. As it can be seen from Table 3, the ANOVA of the regression model (6) showed that quadratic model for Response1 is not rather significant: Fisher *F*-test is very low with a rather high probability value. It is worth of noting that even tabulated *F*-value ($F_{0.05,5,3}$ = 9.01) is higher than calculated *F*-value at the 5% level. Generally, the generated model for the predicting "pseudo"-first-order rate of *p*-CP decay has not high significance, simultaneously possessing rather low regression coefficients (both R^2 = 0.8465 and $R^2_{adj} = 0.5906$). The results in Fig. 1 present the Pareto chart (A) and 3D surface plot (B) for Response1. In Pareto chart the length of each bar indicates the standardized effect of that factor in quadratic model (6) on the response. As it can be observed from Fig. 1(A) only length bar of model component X_2^2 exceeds the reference line which indicate significance on degradation rate of *p*-CP. Thus, it seems that the model failed to capture some relevant factor into consideration, providing the low significance according to the obtained ANOVA results and regression coefficients. However, the results presented in Fig. 1(B) and Table 1 are highly supported by the literature findings [18,19,48]. One can see that the highest rate of *p*-CP decay is observed in the experiments conducted at initial pH 7 and [H_2O_2] = 100 mM. According to the model prediction, the fastest degradation of *p*-CP should occur in weak basic area (pH 9) and the same oxidant concentration, but the similar value of the rate constant is predicted for pH 7. Such model results are in accordance with the findings of Lipczynska-Kochany [48] who studied phenol oxidation by the UV/H_2O_2 process and observed no significant influence of pH on phenol degradation within the range from 7 to 9, while phenol degradation efficiency decreased rapidly at values pH < 7 and pH > 9. Also, the direct photolysis of phenol is accelerated in alkaline solutions due to the increase in "phenolate anions light absorbency" [18]. Accordingly, the findings from our previous study showed that the photolysis combined with H_2O_2 was the most effective for degradation of phenol compounds in weak basic conditions [19]. It is worth of noting that the influence of initial pH on the rate of *p*-CP decay is less pronounced in comparison to the oxidant concentration, i.e. pollutant/oxidant ratio. From Table 1 it can be seen that both observed and predicted values of the rate constant of *p*-CP decay are highest at oxidant concentration of [H_2O_2] = 100 mM at each of the three investigated values of initial pH.

Since the model for Response1, i.e. decay rate of *p*-CP yielded poor results, TOC removal was considered as a second available response influenced by initial pH and pollutant/oxidant ratio in UV/H_2O_2 process. When estimating the influence of operating parameters on overall efficiency of the treatment process for wastewater containing organic pollutants, TOC removal representing mineralization extent of *p*-CP and its by-products is even more eligible response than the conversion of parent pollutant, i.e. rate of *p*-CP decay.

It is known that by oxidative degradation of *p*-CP some by-products, contributing to the TOC content, that are more toxic than parent compound could be formed [4]. Hence, the same Box–Behnken design was applied in order to predict the Response2, TOC removal. The observed and predicted values are given in Table 1, while the second-order polynomial equation presenting the relationship between Response2 and studied process parame-

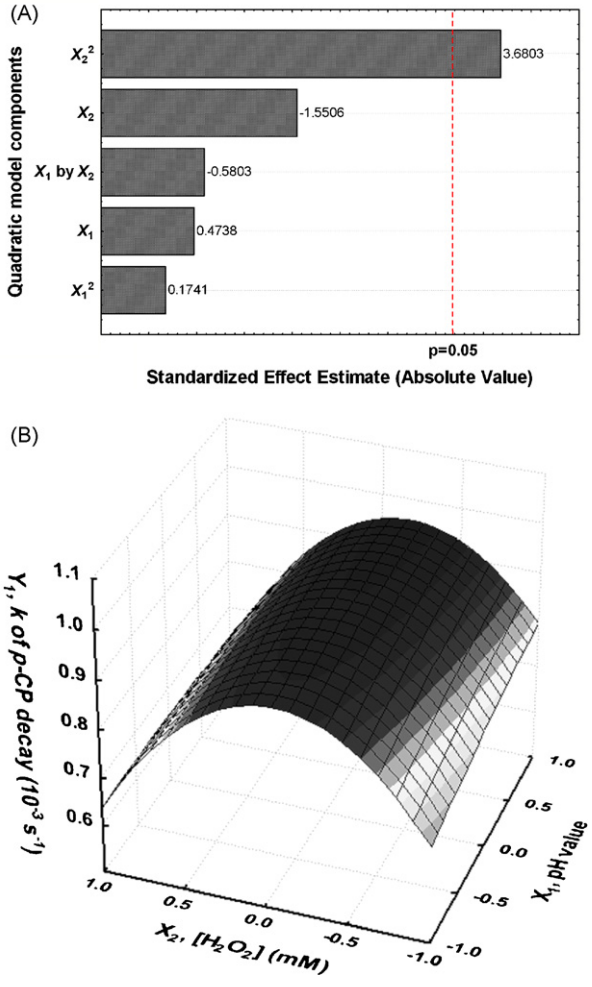

Fig. 1. Graphical presentations for Response1, "pseudo"-first-order rate (k) of *p*-CP decay ($\times 10^{-3}$ s^{-1}): Pareto chart (A) and 3D response surface diagram (B).

ters is given by following Eq. (7).

$$Y_2 = 0.2608 - 0.0078 \times X_1 - 0.0382 \times X_1^2 - 0.0023 \times X_2 - 0.0897 \times X_2^2 + 0.0013 \times X_1 X_2 \quad (7)$$

According to the performed ANOVA, better results are obtained for Response2 (Table 4) than for previously discussed Response1 (Table 3). The Fisher *F*-test is much higher than for previous model, and the probability value less than <0.05 is obtained giving this model satisfactory significance. That can be also confirmed with the comparison for the *F*-calculated and *F*-tabulated: 9.7 (F_{cal}) > 9.01 ($F_{tab\text{-}0.05,5,3}$) as well as by rather high values of regression coefficients (R^2 = 0.9364 and R^2_{adj} = 0.8304). According to Liu et al. [45] the normal probability plot of the residuals is an important diagnostic tool to detect and explain the systematic discrepancies from the assumptions that errors are normally distributed and are independent of each other and that the error variance are homogeneous. Hence, such plot summarizing our results for the prediction of Response2 is presented in Fig. 2(A). One can see that there are no serious violations in the assumptions underlying the analysis. Observing the graphical estimation *vs.* normal distribution on right axes *y*, which is satisfactory enough, one can conclude that residuals are independent [45]. Pareto chart presented in Fig. 2(B) indicated again that the same factor like in previous model (6), X_2^2, posses the highest significance on the response. On the basis of 3D surface plot (Fig. 2(C)), one can clearly observe that neutral pH and H_2O_2 concentration of closely to 100 mM provides the highest TOC removal. The same or very similar conditions are marked in literature as the optimal for the mineralization of wastewater loaded by phenolic compounds [17–19]. At the end, it should be pointed out that, although the model (6) can be marked as not enough significant, in combination with model (7) some valuable information could be drawn. From Figs. 1(B) and 2(C) it can be seen that concentration of H_2O_2 has much higher influence on final responses, either *p*-CP degradation rate or final TOC removal, than initial pH value. Such conclusion on the basis of graphical estimation given in both 3D surface response graphs can be supported with the theory, but experimental studies as well. In theory, the increase of H_2O_2 concentration in the UV/H_2O_2 process could provide benefit to system oxidation power up to certain point, where the further increase has negative influence lowering the concentration of OH radicals available for degradation of organics throughout side reactions with H_2O_2 in excess (reactions #2 and 13, Table 2) [13,18,19]. On the other hand, experimental studies showed that operating pH, especially in this tight range investigated in this study, does not play such significant role. However, somewhat better results are obtained at neutral or weak basic pHs [4,16–19,48]. For the purpose of further study of the kinetic of *p*-CP degradation by UV/H_2O_2 process, the objective of performed RSM is attained. The optimal process conditions are found to be in coded values $X_1 = -0.1023$ and $X_2 = -0.0136$ (uncoded pH 6.8 and [H_2O_2] = 99.32 mM according to the calculations proposed by Yetilmezsoy et al. [26]), predicting the highest TOC removal of 26.12% after 60 min of treatment. After determining the optimal conditions, the study was continued with the development of detail kinetic model describing *p*-CP degradation. Such model includes not only the conversion of *p*-CP and the formation and consequent degradation of aromatic and aliphatic by-products, but also the prediction behavior of some process parameters, e.g. pH changes and H_2O_2 consumption.

4.2. Kinetic modeling

In order to take into account the contribution of direct photolysis in the mathematical model describing the degradation of *p*-CP by UV/H_2O_2 process (M1), the auxiliary model M2 was first developed on the basis of above explained semiempirical "LL model" (Eq. (3)).

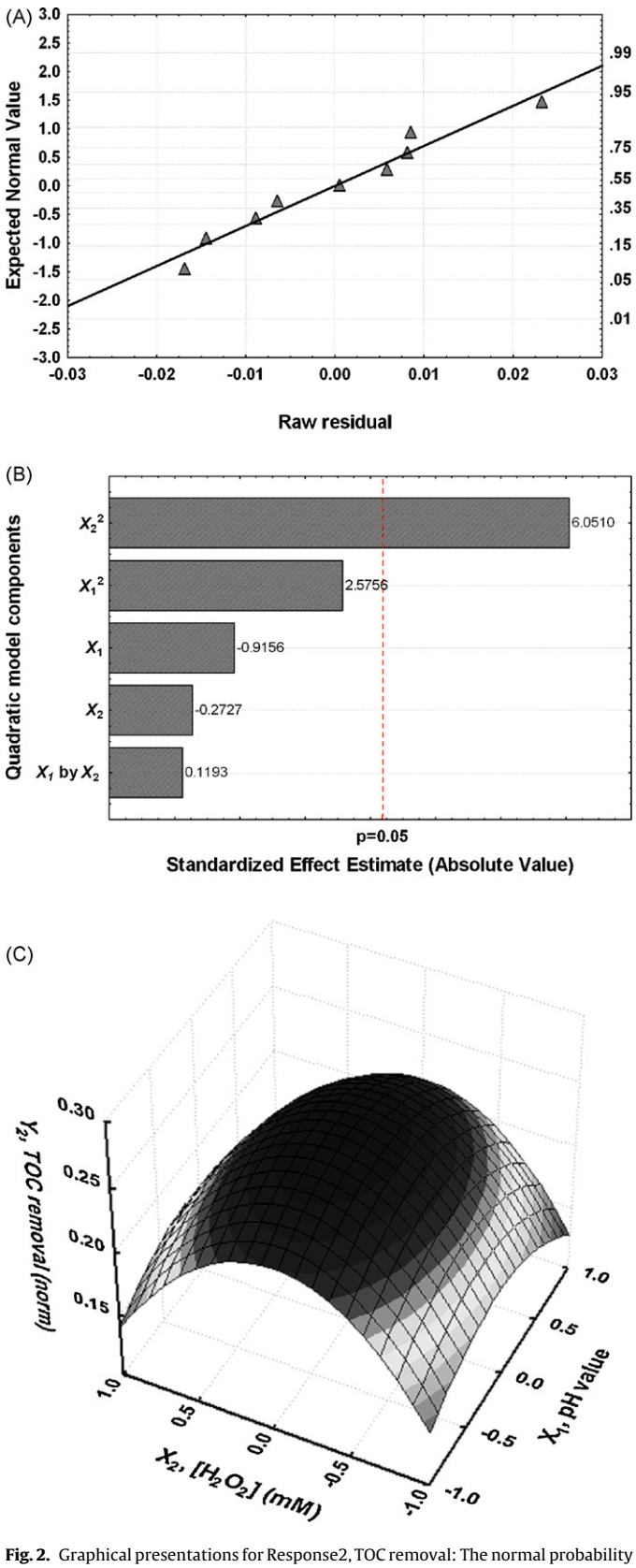

Fig. 2. Graphical presentations for Response2, TOC removal: The normal probability of the raw residuals (A), Pareto chart (B) and 3D response surface diagram (C).

The modified version of "LL model" presented by Eq. (4) was used to describe the degradation of organic compounds present in the system; *p*-CP and its degradation by-products. In such manner the set of ordinary differential equations, presenting the degradation of *p*-CP as a parent pollutant and the formation and subsequent degra-

Table 5
Values of calculated standard deviation (SD) for each of model–experiment data pairs presented in Figs. 4, 5, 7 and 8.

SD × 10^{-2}												
p-CP	4Cl-CC	HQ	MaleAc	FumAc	MaloAc	OxAc	FoAc	UnBP	ArBP	AlBP	IP	H_2O_2
M2 ("auxiliary" model) (UV process, [*p*-CP]$_0$ = 0.5 mM, pH 6.8)												
1.09	0.07	0.69[a]	0.17	–	–	–	1.70	–	–	0.09	–	
M1 ("detail" model) (UV/H_2O_2 process, [*p*-CP]$_0$ = 0.5 mM, [H_2O_2]$_0$ = 99.5 mM, pH 6.8)												
0.53	0.28	0.19	0.25	0.02	0.65	0.89	0.69	0.94	0.32	0.81	0.43	0.16
M3 ("sum" model) (UV/H_2O_2 process, [*p*-CP]$_0$ = 0.5 mM, [H_2O_2]$_0$ = 99.5 mM, pH 6.8)												
0.53	–	–	–	–	–	–	–	–	1.03	2.15	0.89	0.16
M1 ("detail" model) (UV/H_2O_2 process, [*p*-CP]$_0$ = 1.0 mM, [H_2O_2]$_0$ = 99.5 mM, pH 6.8)												
0.23	1.19	0.59	–	–	–	–	–	–	–	–	0.30	–
M1 ("detail" model) (UV/H_2O_2 process, [*p*-CP]$_0$ = 0.5 mM, [H_2O_2]$_0$ = 150 mM, pH 5)												
0.67	1.40	0.84	–	–	–	–	–	–	–	–	0.88	–
M1 ("detail" model) (UV/H_2O_2 process, [*p*-CP]$_0$ = 0.5 mM, [H_2O_2]$_0$ = 50 mM, pH 9)												
2.56	0.58	0.30	–	–	–	–	–	–	–	–	1.05	–

[a] Including formed benzoquinone.

dation of its monitored by-products, was allocated to the system. The degradation of organic pollutants (OP) by direct UV photolysis can be generally presented by known mechanism:

$$\mathrm{OP} \overset{h\nu}{\longleftrightarrow} \mathrm{OP}* \overset{h\nu}{\longrightarrow} \text{products} \quad (8)$$

The role of possibly formed radical species, mainly OH radicals [30,35], was not considered in UV process. As it was mentioned above, the extinction coefficients (ε) and quantum yields (Φ) for each compound detected in the system during *p*-CP degradation by UV process were determined by combining experimental and modeling approach in the following manner. First the ε values of each compound were calculated using results obtained by spectrophotometrical measurements at 254 nm for solutions of pure compounds and well-known method described in our previous research [20]. The solutions were prepared in much higher concentrations than those detected in experiments (>2 mM) in order to minimize the influence of possible formation of by-products. The results are then inserted in the following Eq. (9) [35]:

$$c_{io} - c_i - \frac{1}{\xi} \ln\left[\frac{1-\exp(-\xi c_{io})}{1-\exp(-\xi c_i)}\right] = \Phi_i I_o t \quad (9)$$

being $\xi = 2.303 \times \varepsilon_i \times L$

and the values of quantum yields for each compound were calculated. In such manner the values of Φ for *p*-CP, 4Cl-CC, HQ, MaleAc, FumAc and OxAc are calculated (Table 2). These auxiliary experiments elucidated several important issues regarding the behavior of the studied system. It was found out that maleic acid when illuminated by UV light formed proportional amount of fumaric acid and *vice versa*; these two compounds behave as stereo-isomers when illuminated. Furthermore, it was found out that HQ was degraded to BQ and FumAc, while degradation of 4Cl-CC presumably led to the formation of the unidentified open-ring by-products. It should be pointed out that the experiments of degradation of *p*-CP by UV process in the absence of oxidant was conducted at initial pH 6.8, which was chosen as optimal initial pH for the degradation of the same organic pollutant by UV/H_2O_2, according to the above presented results of performed experimental design. The comparison of the experimental data and those predicted by auxiliary model M2 for *p*-CP degradation by UV process is presented in Fig. 3. In Fig. 3(A) the profiles of *p*-CP decay as well as formation/degradation of detected aromatic by-products 4Cl-CC and HQ, are presented. It should be noted that in this case HQ stands for quinone, (HQ + BQ), where BQ yields with less than 5% in total quinone concentration. Fig. 3(B) summarizes the results of formation/degradation of aliphatic by-products (FumAc and MaleAc), unidentified by-products and mineralized organics expresses as inorganic products, IP. From the results presented in Fig. 3, it can be observed that *p*-CP was degraded only partially, forming mostly the HQ and some unidentified by-products, while other detected

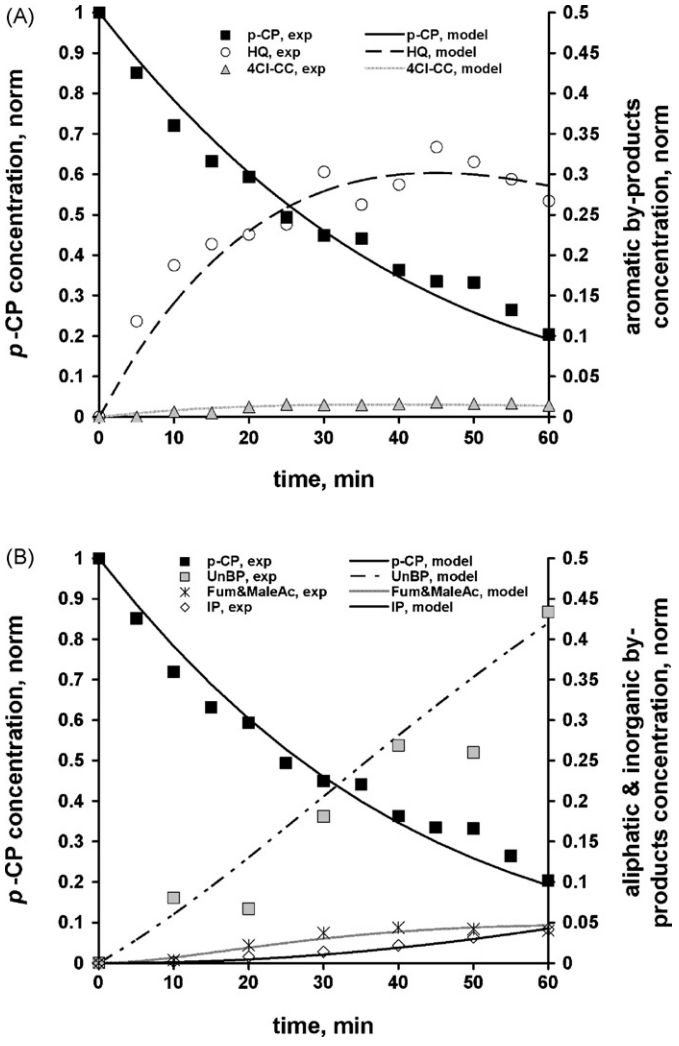

Fig. 3. Degradation of *p*-Chlorophenol in water matrix by UV process. The comparison of experimentally obtained and model predicted data: *p*-CP and formed aromatic by-products (A), aliphatic and unidentified by-products, and mineralization (B) ([*p*-CP]$_0$ = 0.5 mM, pH 6.8).

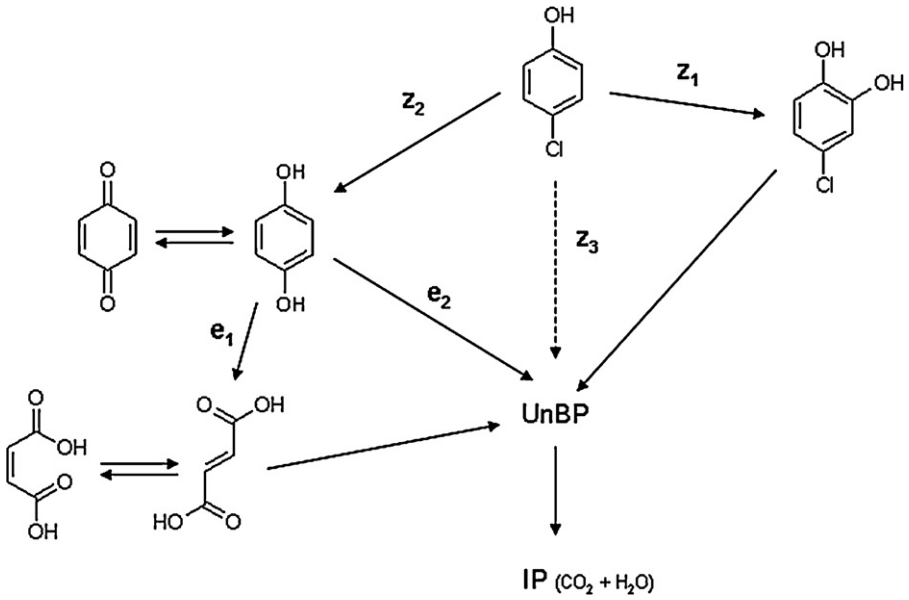

Fig. 4. Pathway of *p*-Chlorophenol degradation used for development of kinetic model for UV process.

by-products amounts less than 5% regarding the initial *p*-CP concentration. Good agreement of experimental and model data is confirmed by rather low values of calculated standard deviation (SD) for each *experimental data*/*model data* pairs (Table 5). Since the degradation of *p*-CP as a parent molecule led mostly to the formation of HQ and small amounts of 4Cl-CC, in order to evaluate the fractions pertaining to each of detected by-products as well as to sum of unidentified by-products, and fit the model to experimental data, several fraction coefficients were introduced. The used fraction coefficients in M1 are marked with z (z_1, z_2 and z_3) presenting the fractions of *p*-CP degraded to HQ, 4Cl-CC and unidentified by-products, respectively, as presented in Fig. 4. The proposed degradation pathway of *p*-CP by UV process was based on known OH radicals degradation mechanism which was correlated with identified and unidentified *p*-CP degradation by-products. Hence, it is known that in the first step *p*-CP is degrading to HQ and 4Cl-CC and then further to three-substituted-phenols and to ring-opened products [8]. In such manner, accordingly to the results presented at Fig. 3(A) as well as those obtained in auxiliary experiments where Φ for HQ was calculated, the fraction coefficients e_1 and e_2 are contributed to fractions of HQ degraded to FumAc and unidentified by-products, respectively. The values of z and e coefficients, are calculated using trial and error method by choosing the number automatically between 0 and 1, satisfying the rule that their sum should be equal to 1 (e.g. $z_1 + z_2 + z_3 = 1$) with simultaneous comparison by experimentally obtained data fitting the model curve to them using the mathematical expression that SD values should gravitate to minimum built in used IF-loop. Hence, the calculated values of fraction coefficients obtained real values ($z_1 = 0.043$, $z_2 = 0.726$, $z_3 = 0.231$, $e_1 = 0.522$, $e_2 = 0.478$) correlating closely empirical results with developed auxiliary model M2 (Fig. 3 and Table 5), and were used in development of detail mathematical model M1.

Once the optimal operating parameters are determined by the means of experimental design and model M2 describing *p*-CP degradation by direct photolysis was successfully developed we approached to the development of the detail mathematical model M1 describing the system behavior during the *p*-CP degradation by UV/H_2O_2 process. The process was performed at above established operating conditions, pH 6.8 and pollutant/oxidant ratio 1:199, i.e. [H_2O_2] = 99.5 mM, yielding with the results presented in Fig. 5. It should be pointed out that 27.03% of TOC removal was obtained after 60 min of treatment, which is very close to the value predicted by RSM (26.12% TOC removal). The results of *p*-CP degradation and formation/degradation of monitored aromatic by-products are shown in Fig. 5(A), the profiles of formation/degradation of monitored aliphatic by-products are presented in Fig. 5(B), while the formation/degradation of unidentified by-products, mineralization and the changes pH and H_2O_2 concentration are summarized in Fig. 5(C), all compared with the corresponding predictions obtained by model M1. According to the calculated SD values ranging from 0.0002 to 0.0094 (Table 5), one can conclude that M1 describes system behavior with rather high accuracy. A slight discrepancy between model and experimental data can be observed only in the case of pH values. Although the trend of the curve for predicted pH valued follows experimental data, the drop in pH predicted by model is somewhat more pronounced than that obtained by the experiment (Fig. 5(C)). In model development, the pathway of *p*-CP degradation by OH radicals proposed by Zhou et al. [8] was combined with those of phenol by OH radicals, especially regarding the formation of aliphatic by-products, as proposed by Shen et al. [49] and Pimentel et al. [50]. The proposed pathway of *p*-CP degradation by UV/H_2O_2 process used in the model development is presented in Fig. 6. According to Zhou et al. [8] *p*-CP degrades primarily to HQ and 4Cl-CC, with the subsequent formation of various ring-opened products. Several possible aliphatic by-products of *p*-CP degradation were monitored (listed in Section 2) and among them only MaleAc, FumAc, MaloAc, OxAc and FoAc were detected and thereafter considered in proposed pathway. All other possible by-products were summarized under the term unidentified by-products, but it should be pointed out that their sum concentration amounts less than 10% of initial *p*-CP concentration with decreasing tendency toward 0% when treatment time approached 60 min (Fig. 5(C)). The significant and valuable information regarding the formation and degradation of detected aliphatics in the system were acquired from work of Pimentel et al. [50]. They proposed pathways of several aliphatic precursors (carboxylic acids) providing their predominant degradation by-products. Hence, maleic acid degrades predominately to oxalic and formic acid. The same as is valid for fumaric acid, while malonic acid decomposes only to oxalic acid. Furthermore, oxalic and formic degrade to inorganic products (IP), i.e. to CO_2 and H_2O. These findings were taken into

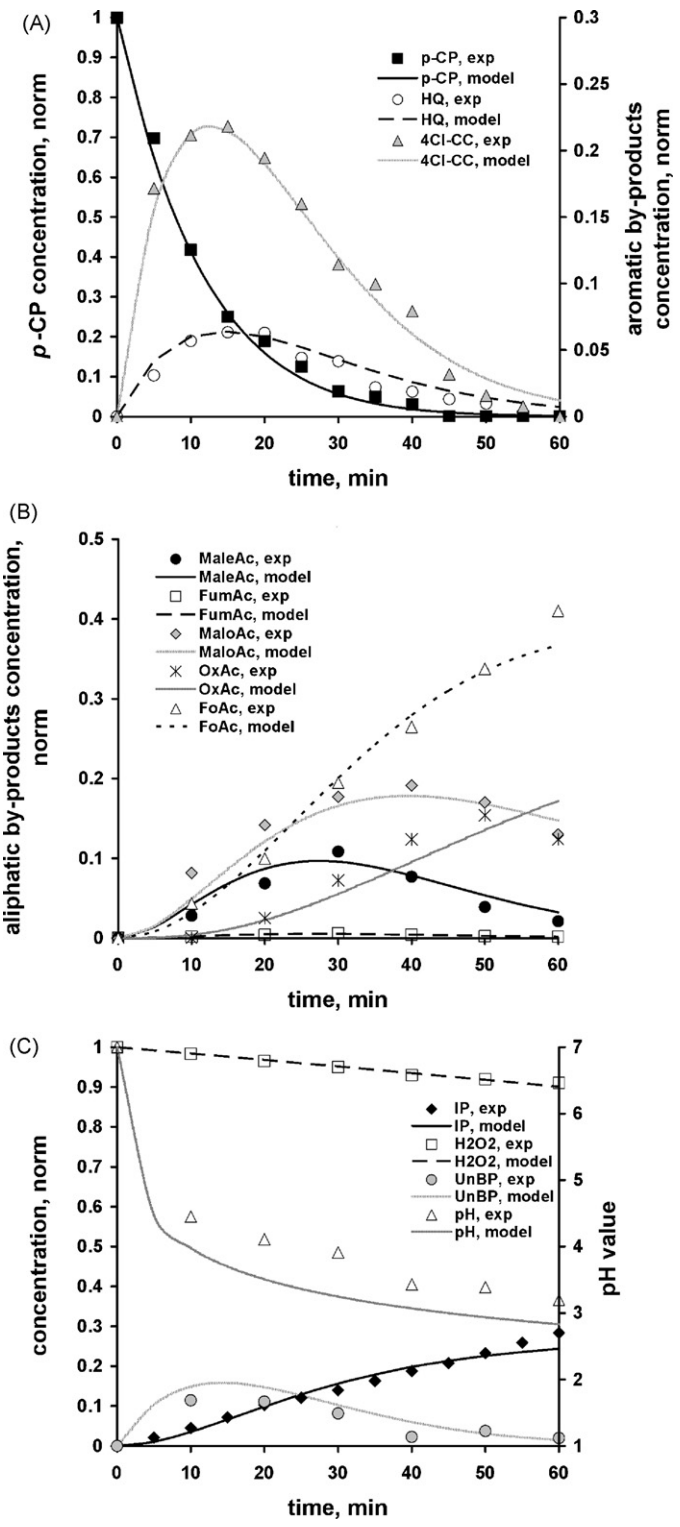

Fig. 5. Degradation of *p*-Chlorophenol in water matrix by UV/H_2O_2 process. The comparison of experimentally obtained and data predicted by "detail" model: *p*-CP and formed aromatic by-products (A), aliphatic by-products (B) and unidentified by-products, mineralization, H_2O_2 consumption and pH (C) ([*p*-CP]$_0$ = 0.5 mM, [H_2O_2]$_0$ = 99.5 mM, pH 6.8).

account when fraction coefficients are contributed to the particular organic compounds identified and monitored in our study. Besides fraction coefficients *e* and *z*, which are built-in alongside the auxiliary model M2 in this main model M1 describing the behavior of UV/H_2O_2 process, several new coefficients are estimated using the above described trial and error method run automatically within the set IF-loop in program syntax in order to obtained satisfactory fitting of model and empirical data. Hence, the values of following fraction coefficients are determined: $q_1 = 0.601$, $q_2 = 0.082$ and $q_3 = 0.317$ describing the degradation of *p*-CP by OH radicals to 4Cl-CC, HQ and UnBP, respectively; $w_1 = 0.519$, $w_2 = 0.001$ and $w_3 = 0.480$ describing the degradation of both HQ and 4Cl-CC by OH radicals to MaleAc, FumAc and MaloAc, respectively; $n_1 = 0.122$ and $n_2 = 0.878$ describing the degradation of both MaleAc and FumAc by OH radicals to OxAc and FoAc, respectively; and $m_1 = 0.002$, $m_2 = 0.401$ and $m_3 = 0.597$ presenting the fractions of unidentified by-products degraded to OxAc, FoAc and IP. It should be pointed out that besides known rates of reactions of each monitored compound and OH radicals used in model development (Table 2), the rate of reaction #32 (Table 2) was determined using trail and error method. The order of magnitude of the obtained value, 6.83×10^9 M^{-1} s^{-1}, is in accordance with the values reported in the literature for phenolic compounds and their by-products, both aromatic and aliphatic with higher molecular weight which can be assumed to constitute these unidentified by-products [8,14,18,20,31,32,36–39,43]. It is also worth of noting that, although pathways of *p*-CP degradation (Figs. 4 and 6) are similar in the first stage when by-products HQ and 4Cl-CC are generated, their proportion is different. Namely, when UV process is applied, significantly higher amount of HQ in comparison to 4Cl-CC is formed by degradation of *p*-CP. On the other hand, in the case of UV/H_2O_2 process this proportion is quite opposite and much higher amount of 4Cl-CC is formed in comparison to HQ. Concerning the rather high toxicity of HQ toward several microorganisms [51,52], this issue is of particular importance when AOPs, particularly UV/H_2O_2 process, are combined with sequential biological treatment is considered for the treatment of wastewater containing chlorinated phenols.

For some practical purposes, the rough estimation of system behavior might provide sufficient information on potential performance of oxidative treatment system. Hence, besides previously described detail mathematical model M1, the simplified "sum" model M3, was developed. In this model only reactions of *p*-CP and its summarized aromatic (ArBP) and aliphatic (AlBP) by-products both with OH radicals are considered. Such simplified degradation mechanism is presented by Eq. (5). The results of experimentally obtained data are compared with the data predicted by both M1 and M3 model, Fig. 7(A) and (B), respectively. In this purpose, model M1 was set to predict sum-products for the group of compounds: ArBP and AlBP by simply summarizing their estimated concentration, with the assumption that UnBP pertain to AlBP. In such manner the model M1 provided close matching of predicted values with sum of empirically obtained values for ArBP and AlBP (Fig. 7(A); SD values ranged from 0.0043 to 0.0081 (Table 5). In model M3 the rate constants of reactions #33 and 34 were estimated, by the means of earlier described trial and error method. It can be seen that obtained values, 6.25×10^9 M^{-1} s^{-1} and 5.83×10^8 M^{-1} s^{-1} for reactions #33 and 34, respectively, corresponds by the order of magnitude to reaction rate constants of particular compounds constituting the group parameters (ArBP and AlBP) (Table 2). Moreover, in the case of ArBP the determined value of reaction rate constant (#33) is close to the arithmetic mean of values of reaction rate constants for HQ (#23) and 4Cl-CC (#21), 5.2×10^9 M^{-1} s^{-1} and 7.0×10^9 M^{-1} s^{-1}, respectively. Although results of "sum" model M3 do not match so closely with empirical results (Fig. 7(B)) in comparison to those obtained by "detail" model M1 (Fig. 7(A)), trends of aromatic and aliphatic formation and their subsequent degradation provide rough estimation of system behavior.

In order to evaluate predictivity of detail model M1, its performance was tested for the prediction of system behavior observing *p*-CP degradation, the formation/degradation of its aromatic by-products HQ and 4Cl-CC, as well as mineralization extent of

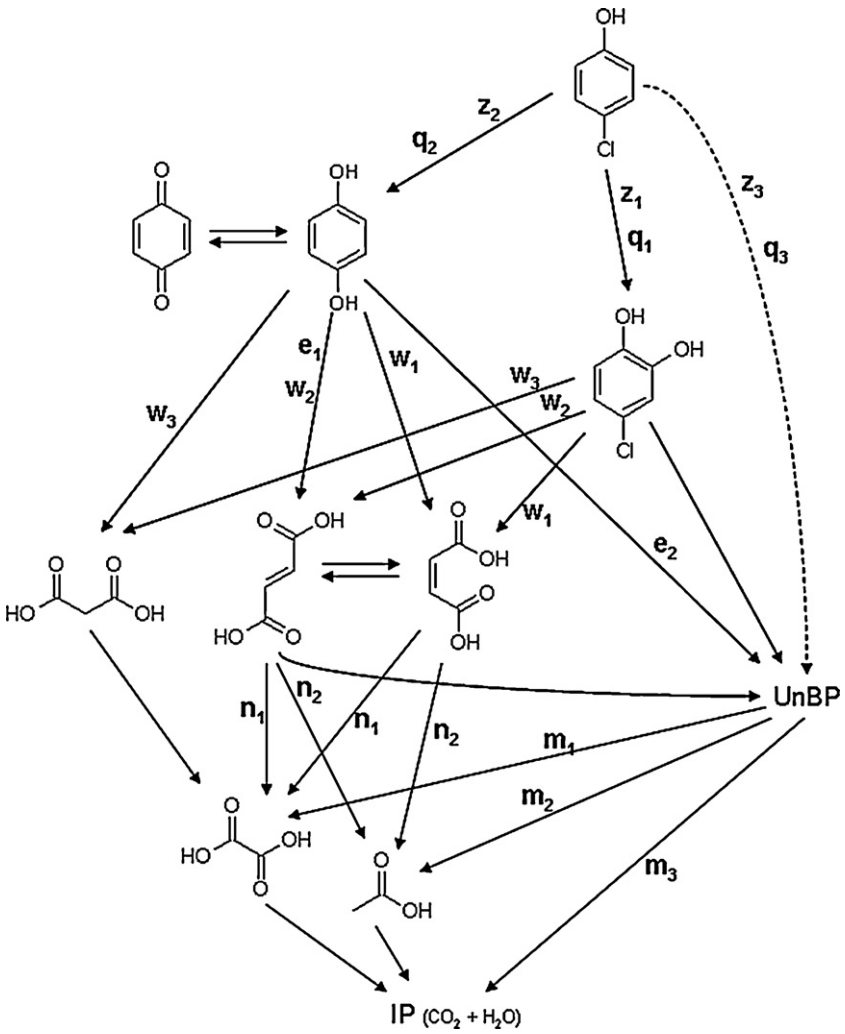

Fig. 6. Pathway of *p*-Chlorophenol degradation used for development of "detail" kinetic model for UV/H_2O_2 process ($[p\text{-CP}]_0$ = 0.5 mM, $[H_2O_2]_0$ = 99.5 mM, pH 6.8).

simulated wastewater, when UV/H_2O_2 process was applied at different processes conditions; initial [*p*-CP] pH and pollutant/oxidant ratio. The comparison of experimental and model data is presented in Fig. 8. Hence, in Fig. 8(A) are presented the results obtained for twice as high initial *p*-CP concentration ($[p\text{-CP}]_0$ = 1 mM) as that used in model developing (Fig. 5), while values of initial pH (pH 6.8) and ratio $[p\text{-CP}]_0/[H_2O_2]_0$ = 1:199 were the same as determined as optimal using RSM. In Fig. 8(B) and (C) are presented results obtained for the same initial *p*-CP concentration ($[p\text{-CP}]_0$ = 0.5 mM) as in model development, while the initial pH and initial pollutant/oxidant ratio were altered (pH 5 and $[p\text{-CP}]_0/[H_2O_2]_0$ = 1:300 in Fig. 8(B) and pH 9 and $[p\text{-CP}]_0/[H_2O_2]_0$ = 1:100 in Fig. 8(C)). One can see that "detail" model M1 described satisfactory the system behavior, predicting the trends of degradation and formation/degradation for monitored organics, while only slight discrepancies from empirical data points could be observed in some cases. According to the calculated SD values it can be concluded that M1 predict system behavior with rather good accuracy in the case of higher *p*-CP concentration (Fig. 8(A)) as well as in the case when the process is operated at pH 5 and higher pollutant/oxidant ratio (Fig. 8(B)). Calculated SD values ranged from 0.0023 to 0.0119 and from 0.0067 to 0.0140, respectively (Table 5). In the case when the process is operated at pH 9 and lower pollutant/oxidant ratio (Fig. 8(C)) somewhat faster *p*-CP degradation was predicted by model M1 in comparison to experimentally obtained results. However, curves predicting the formation/degradation of direct products of *p*-CP degradation, HQ and 4Cl-CC fit empirical data points. It should be pointed out that since it was evidenced that the rate of *p*-CP degradation by OH radicals depends on operating pH range [36,37], in the evaluation of model M1 it was assumed that the pathway of *p*-CP degradation is influenced as well (Fig. 8(B) and (C)). Hence, the fraction coefficients for the formation of aromatic by-products HQ and 4Cl-CC, as well for UnBP (q_1, q_2, and q_3) which are marked as direct by-products of *p*-CP degradation (Fig. 6) were set to adjust automatically using the trail and error method built in model IF-loop. Although it could be assumed that the rate of direct photolysis of *p*-CP and the subsequent formation of aromatic by-products monitored is also pH depended, these factors were not taken into consideration in the model evaluation (*z* fraction coefficients were kept the same as determined in auxiliary model for UV process) due to its complexity and the fact that OH radical mechanism prevails over direct photolysis in UV/H_2O_2 process [17,18,30]. The other fraction coefficients were also kept at earlier determined values due to the fact that other organic compounds were not monitored in the model evaluation and we did not want to speculate the changes in their formation/degradation. Accordingly, the fraction coefficient for the formation of 4Cl-CC by *p*-CP degradation at pH 9 obtained somewhat higher value q_1 = 0.673, while in the case of pH 5 value q_1 = 0.598 was match closely to that for pH 6.8 (q_1 = 0.601). Similarly, new values of fraction coefficient for HQ were obtained; q_2 = 0.185 for process at pH 5 (Fig. 8(B)), and q_2 = 0.078 at pH 9 which was very close to one obtained for

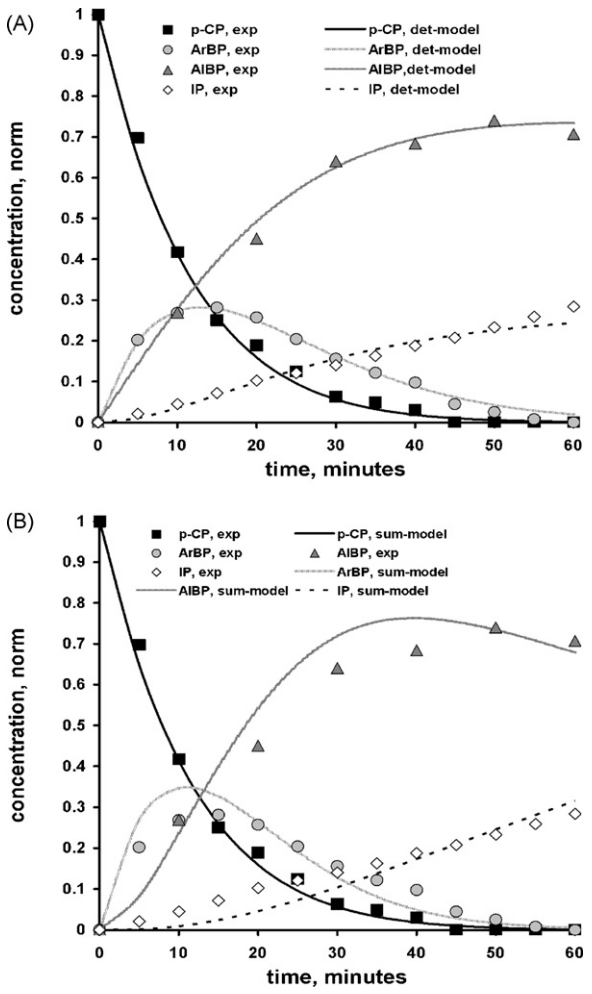

Fig. 7. Degradation of *p*-Chlorophenol in water matrix by UV/H_2O_2 process. The comparison of sum-data (aromatic, aliphatic and inorganic products) predicted by "detail" (A) and "sum" model (B) ([*p*-CP]$_0$ = 0.5 mM, [H_2O_2]$_0$ = 99.5 mM, pH 6.8).

process operated at neutral pH (q_2 = 0.082). As a consequence of these changes in the fraction coefficients for 4Cl-CC and HQ formation, new values of fraction coefficients of UnBP were calculated for both pHs; q_3 = 0.217 for pH 5 and q_3 = 0.249 for pH 9. On the basis of these results, as well the empirical values of monitored by-products of *p*-CP degradation it can be concluded that at mild acid conditions dechlorination of benzene ring and its subsequent hydroxylation in *para* position is more favored than at neutral and weak basic conditions. Similarly, the hydroxylation of benzene ring in *ortho* position and production of 4Cl-CC as by-product of *p*-CP degradation by OH radicals is more favored at weak basic than at neutral and mild acidic conditions. These findings provide very useful information on the pathways directions and the yield of reactions, which is particularly important for studying the toxicity of wastewaters and the possibility to combine AOPs with sequential biological treatment, as it was already mentioned above.

At the end, it is worth of noting that the performance of developed model M1 was tested in order to predict only the mineralization of overall organic content (OC) of simulated *p*-CP wastewater concerning only the sum reaction #35 (Table 2) as relevant for the consumption of OH radicals in reactions with organic species, while all other reactions incorporated in model describing the reactions between inorganic species were kept the same (reactions from #1 to 17, Table 2). The rate constant of reaction #35, $k_{35} = 2.22 \times 10^8\ M^{-1}\ s^{-1}$, was determined by trail and error method providing almost the perfect fitting of model results to empirical

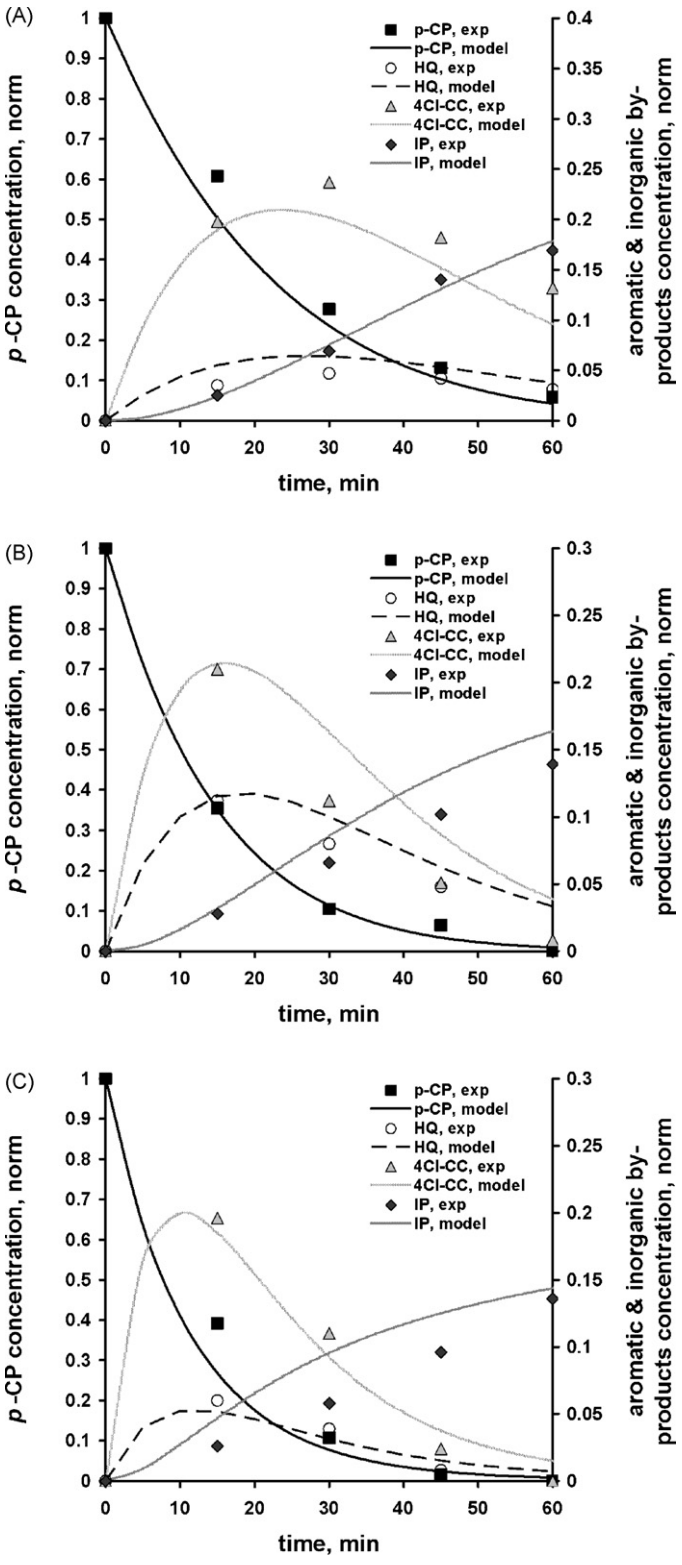

Fig. 8. Degradation of *p*-Chlorophenol in water matrix by UV/H_2O_2 process. The comparison of *p*-CP degradation, formed aromatic by-products and mineralization experimentally obtained and predicted by "detail" model at different process conditions: [*p*-CP]$_0$ = 1.0 mM, [H_2O_2]$_0$ = 99.5 mM, pH 6.8 (A); [*p*-CP]$_0$ = 0.5 mM, [H_2O_2]$_0$ = 150 mM, pH 5 (B); [*p*-CP]$_0$ = 0.5 mM, [H_2O_2]$_0$ = 50 mM, pH 9 (C).

ones (results were not showed, calculated SD = 0.0047). This test was performed in order to compare obtained value k_{35} with the rate constant of reaction for mineralization of OC in the case of phenol model wastewater when treated by Fenton type process ($k_{OC} = 2.33 \times 10^8\ M^{-1}\ s^{-1}$), determined in our previous study [20].

The rate of such overall reaction is considered to be dependent on complexity of chemical structure of overall organics present in the system, while it is worth of noting that phenol degradation by-products are very similar to those of *p*-CP degradation [8,49,50]. Hence, the value of k_{35} obtained in this study, corresponding closely to that from previous study on phenol [20], provides further evidence that developed model M1 may be classified as transparent, flexible and accurate in prediction of the behavior of system with predominant OH radical mechanism for oxidative degradation of organic pollutants in water.

5. Conclusions

The aim of the study was to developed detail mathematical model describing the degradation of chlorinated hydrocarbon pollutants by UV/H_2O_2 process. Since all AOPs, and among them UV/H_2O_2 process, are multifactor systems, in order to avoid misinterpretations on system behavior obtained observing only single-factor effects which could influence the final goal of the study; the model predicting kinetic of degradation of chosen pollutant, the influence of cross-factor effects of process parameters was investigated as well. Hence, in order to establish the optimal operating parameters of UV/H_2O_2 process influencing the treatment efficiency, such as pH range of application and oxidant concentration, the two-factors three-level Box–Behnken experimental design combined with response surface modeling (RSM) and quadratic programming was successfully applied. The results of such experimental design using different statistical tools showed that neutral pH (more precisely 6.8) and pollutant/oxidant ratio 1:199 are the most suitable to maximize the oxidative power of treatment system. On these optimal conditions was performed experimental part of the study in order to obtained empirical values crucial in model development. In model development were included both mechanisms describing (i) *p*-CP degradation taking into account reactions occurring in the bulk between inorganic and organic species (*p*-CP and its degradation by-products and OH radicals) as well (ii) so-called bulk inorganic reactions including reactions between radical, ionic and molecular species present in the system. The model accuracy was tested in order to predict system behavior at different process conditions and pollutant concentrations, providing rather good fitting of model results to empirical ones, which was confirmed by calculated values of standard deviation for each experimentally monitored parameter; organic species, mineralization, changes of pH and H_2O_2 consumption.

Hence, it can be concluded that the developed mathematical model describing the degradation kinetic of *p*-CP by UV/H_2O_2 process can be characterized as interpretable, flexible and accurate, and can be considered as a base for future studies with the aim of maximizing efficiency of wastewater treatment by AOPs.

Acknowledgements

We would like to acknowledge the financial support both from the Ministry of Science, Education and Sport, Republic of Croatia (Project #125-1253092-1981) and the National Foundation for Science, Higher Education and Technological Development of the Republic of Croatia (Project #04/14, *Wastewater Treatment in DINA-Petrokemija Omisalj as a Contribution to Ecosystem Preservation*).

References

[1] W.P. Cunningham, M.A. Cunningham, B. Saigo, Environmental Science, a Global Concern, Mc Graw-Hill Education, New York, USA, 2005.
[2] R.A. Meyers, D. Kender Dittrick, The Wiley Encyclopedia of Environmental Pollution and Cleanup, Wiley, New York, USA, 1999.
[3] F.J. Benitez, J. Beltrán-Heredia, J.L. Acero, F.J. Rubio, Rate constants for the reactions of ozone with chlorophenols in aqueous solutions, J. Hazard. Mater. 79 (2000) 271–285.
[4] M. Pera-Titus, V. Garcia-Molina, M.A. Banos, J. Gimenez, S. Esplugas, Degradation of chlorophenols by means of advanced oxidation processes: a general review, Appl. Catal. B 47 (2004) 219–256.
[5] EPA, July 2002, http://www.scorecard.org.
[6] EC Decision 2455/2001/EC of the European Parliament and of the Council of November 20, 2001 establishing the list of priority substances in the field of water policy and amending Directive 2000/60/EC (L 331 of 15-12-2001).
[7] S.G. Poulopoulos, M. Nikolaki, D. Karampetsos, C.J. Philippopoulos, Photochemical treatment of 2-chlorophenol aqueous solutions using ultraviolet radiation, hydrogen peroxide and photo-Fenton reaction, J. Hazard. Mater. 153 (2008) 582–587.
[8] T. Zhou, Y. Li, J. Ji, F.-S. Wong, X. Lu, Oxidation of 4-chlorophenol in a heterogeneous zero valent iron/H_2O_2 Fenton-like system: kinetic, pathway and effect factors, Sep. Purif. Technol. 62 (2008) 551–558.
[9] A.P. Sincero, G.A. Sincero, Physical–Chemical Treatment of Water and Wastewater, CRC Press, IWA Publishing, New York, USA, 2003.
[10] W. Viessman Jr., M.J. Hammer, Water Supply and Pollution Control, 7th ed., Pearson Education, Upper Saddle River, USA, 2005.
[11] S. Parsons, Advanced Oxidation Processes for Water and Wastewater Treatment, IWA Publishing, London, England, 2004.
[12] P.R. Gogate, A.B. Pandit, A review of imperative technologies for wastewater treatment. I. oxidation technologies at ambient conditions, Adv. Environ. Res. 8 (2004) 501–551.
[13] J.C. Crittenden, S. Hu, D.W. Hand, S.A. Green, A kinetic model for H_2O_2/UV process in a completely mixed batch reactor, Water Res. 33 (10) (1999) 2315–2328.
[14] A.K. De, B. Chaudhuri, S. Bhattacharjee, B.K. Dutta, Estimation of •OH radical reaction rate constants for phenol and chlorinated phenols using UV/H_2O_2 photo-oxidation, J. Hazard. Mater. B 64 (1999) 91–104.
[15] J.A. Zimbron, K.F. Reardon, Hydroxyl free radical reactivity toward aqueous chlorinated phenols, Water Res. 39 (5) (2004) 865–869.
[16] F. Al Momani, C. Sans, S. Esplugas, A comparative study of the advanced oxidation of 2,4-dichlorophenol, J. Hazard. Mater. B 107 (2004) 123–129.
[17] S. Esplugas, J. Gimenez, S. Contreras, E. Pascual, M. Rodriguez, Comparison of different advanced oxidation processes for phenol degradation, Water Res. 36 (2002) 1034–1042.
[18] R. Alnaizy, A. Akgerman, Advanced oxidation of phenolic compounds, Adv. Environ. Res. 4 (3) (2000) 233–244.
[19] H. Kusic, N. Koprivanac, A. Loncaric Bozic, Minimization of organic pollutant content in aqueous solution by means of AOPs: UV- and ozone-based technologies, Chem. Eng. J. 123 (3) (2006) 127–137.
[20] H. Kušić, N. Koprivanac, A. Lončarić Božić, I. Selanec, Photo-assisted Fenton type processes for the degradation of phenol: a kinetic study, J. Hazard. Mater. B136 (2006) 632–644.
[21] I. Nicole, J. De Laat, M. Dore, J.P. Duguet, C. Bonnnel, Utilisation du rayonnement ultraviolet dans le traitement des eaux: mesure du flux photonique par actinometrie chimique au peroxyde d'hydrogene (Use of U.V. radiation in water treatment: measurement of photonic flux by hydrogen peroxide actinometry), Water Res. 24 (2) (1990) 157–168.
[22] H. Kusic, Minimization of Organic Content in Colored Wastewaters by the Means of Advanced Oxidation Processes, Thesis (PhD), University of Zagreb, 2006.
[23] L.S. Clesceri, A.E. Greenberg, A.D. Eaton, Standard Methods for the Examination of Water and Wastewater Treatment, 20th ed., APHA & AWWA & WEF, USA, 1998.
[24] E. Bayraktar, Response surface optimization of the separation of DL-tryptophan using an emulsion liquid membrane, Proc. Biochem. 37 (2001) 169–175.
[25] M.Y. Can, Y. Kaya, O.F. Algur, Response surface optimization of the removal of nickel from aqueous solution by cone biomass of *Pinus sylvestris*, Bioresour. Technol. 97 (2006) 1761–1765.
[26] K. Yetilmezsoy, S. Demirel, R.J. Vanderbei, Response surface modeling of Pb(II) removal from aqueous solution by *Pistacia vera* L.: Box–Behnken experimental design, J. Hazard. Mater. 171 (2009) 551–562.
[27] E.V. Rokhina, M. Sillanpää, M.C.M. Nolte, J. Virkutyte, Optimization of pulp mill effluent treatment with catalytic adsorbent using orthogonal second-order (Box–Behnken) experimental design, J. Environ. Monitor. 10 (2008) 1304–1312.
[28] http://www.biokin.com/tools/fcrit.html (September/October, 2009).
[29] http://www.danielsoper.com/statcalc/calc07.aspx (September/October, 2009).
[30] F.J. Beltran, Ozone-UV radiation-hydrogen peroxide oxidation technologies, in: M.A. Tarr (Ed.), Chemical Degradation Methods for Wastes and Pollutants—Environmental and Industrial Applications, Marcel Dekker Inc., New York, USA, 2003, pp. 1–77.
[31] N. Kang, D.S. Lee, J. Yoon, Kinetic modeling of Fenton oxidation of phenol and monochlorophenols, Chemosphere 47 (2002) 915–924.
[32] R. Chen, J.J. Pignatello, Role of quinone intermediates as electron shuttles in Fenton and photoassisted Fenton oxidations of aromatic compounds, Environ. Sci. Technol. 31 (1997) 2399–2406.
[33] H. Gallard, J. De Laat, Kinetic modelling of Fe(III)/H_2O_2 oxidation reactions in dilute aqueous solution using atrazine as a model organic compound, Water Res. 34 (12) (2000) 3107–3116.
[34] D.R. Grymonpre, W.C. Finney, R.J. Clark, B.R. Locke, Suspended activated carbon particles and ozone formation in aqueous phase pulsed corona discharge reactors, Ind. Eng. Chem. Res. 42 (2003) 5117–5134.

[35] O. Gimeno, M. Carbajo, F.J. Beltran, F.J. Rivas, Phenol and substituted phenols AOPs remediation, J. Hazard. Mater. B119 (2005) 99–108.
[36] U. Stafford, K.A. Gray, P.V. Kamat, Radiolytic and TiO_2-assisted photocatalytic degradation of 4-chlorophenol. A comparative study, J. Phys. Chem. 98 (1994) 6343–6351.
[37] R.S. Shetiya, K.N. Rao, J. Shankar, OH-radical rate constants of phenols using *p*-nitrosodimethylaniline, Indian J. Chem. 14A (1976) 575–578.
[38] A.A. Al-Suhybani, G. Hughes, Pulse radiolysis of deaerated hydroquinone solutions, J. Chem. Soc. Pak. 8 (1986) 107–115.
[39] D.E. Cabelli, B.H.J. Bielski, A pulse radiolysis study of some dicarboxylic acids of the citric acid cycle. The kinetic and spectral properties of the free radicals formed by reaction with the OH radical, Z. Naturforsch. B Anorg. Chem., Org. Chem. 40 (1985) 1731–1737.
[40] C. Walling, G.M. El-Taliawi, Fenton's reagent. II. Reactions of carbonyl compounds and alpha, beta-unsaturated acids, J. Am. Chem. Soc. 95 (1973) 844–847.
[41] G. Scholes, R.L. Willson, γ-Radiolysis of aqueous thymine solutions. Determination of relative reaction rates of OH radicals, Trans. Faraday Soc. 63 (1967) 2983–2993.
[42] N. Getoff, F. Schwoerer, V.M. Markovic, K. Sehested, S.O. Nielsen, Pulse radiolysis of oxalic acid and oxalates, J. Phys. Chem. 75 (1971) 749–755.
[43] G.V. Buxton, C.L. Greenstock, W.P. Helman, A.B. Ross, Critical review of rate constants for reactions of hydrated electrons, hydrogen atoms and hydroxyl radicals ($^{\bullet}OH/^{\bullet}O^{-}$) in aqueous solution, J. Phys. Chem. Ref. Data 17 (1988) 513–586.
[44] N. Nirmalakhandan, Modeling Tools for Environmental Engineers and Scientists, CRC Press, New York, USA, 2002.
[45] H.-L. Liu, Y.-W. Lan, Y.-C. Cheng, Optimal production of sulphuric acid by *Thiobacillus thiooxidans* using response surface methodology, Proc. Biochem. 39 (2004) 1953–1961.
[46] J.F. Fu, Y.Q. Zhao, X.D. Xue, W.C. Li, A.O. Babatunde, Multivariate-parameter optimization of acid blue-7 wastewater treatment by Ti/TiO_2 photoelectrocatalysis via the Box–Behnken design, Desalination 243 (2009) 42–51.
[47] R. Sen, T. Swaminathan, Response surface modeling and optimization to elucidate and analyze the effects of inoculum age and size on surfactin production, Biochem. Eng. J. 21 (2004) 141–148.
[48] E. Lipczynska-Kochany, Hydrogen peroxide mediated photodegradation of phenol as studied by a flash photolysis/HPLC technique, Environ. Pollut. 61 (1993) 147–152.
[49] Y. Shen, L. Lei, X. Zhang, M. Zhou, Y. Zhang, Effect of various gases and chemical catalysts on phenol degradation pathways by pulsed electrical discharges, J. Hazard. Mater. 150 (2008) 713–722.
[50] M. Pimentel, N. Oturan, M. Dezotti, M.A. Oturan, Phenol degradation by advanced electrochemical oxidation process electro-Fenton using a carbon felt cathode, Appl. Catal. B 83 (2008) 140–149.
[51] V.L.K. Jennings, M.H. Rayner-Brandes, D.J. Bird, Assessing chemical toxicity with the bioluminescent photobacterium (*vibrio fischeri*): a comparison of three commercial systems, Water Res. 35 (2001) 3448–3456.
[52] P. Calza, C. Massolino, E. Pelizzetti, Photo-induced transformation of hexaconazole and dimethomorph over TiO_2 suspension, J. Photochem. Photobiol., A 200 (2008) 356–363.